# On the Interpretation of Seasonal Southern Africa Precipitation Prediction Skill Estimates during Austral Summer

Andrew Hoell[1]

NOAA/Earth System Research Laboratory Physical Sciences Division

Boulder, CO, USA

Jon Eischeid

NOAA/Earth System Research Laboratory Physical Sciences Division

Cooperative Institute for Research in the Environmental Sciences

University of Colorado Boulder

Boulder, CO, USA

Submitted to *Climate Dynamics*: March 4, 2019

Revised for *Climate Dynamics*: August 8, 2019

[1] Corresponding Author: Andrew Hoell, NOAA/Earth System Research Laboratory Physical Sciences Division, 325 Broadway, Boulder, CO 80305, email: andrew.hoell@noaa.gov

## Abstract

Differences between two types of prediction skill estimates over Southern Africa are illustrated to better inform the users of seasonal precipitation forecasts over the region who desire assessments of forecast accuracy. Both seasonal precipitation prediction skill estimates for the African continent south of 15˚S during the December-March rainy season are derived from the perfect-model method. The perfect-model method is based on a 40-member ensemble of Community Atmosphere Model version 5 simulations forced by observed time-evolving boundary conditions during 1920-2016.

The first skill estimate is based on the verification of an ensemble mean forecast spanning many seasons and therefore unconditional on a single boundary forcing. The second skill estimate is based on the verification of an ensemble mean forecast for a single season and is therefore conditional on that year's boundary forcing. Unconditional prediction skill calculated in 30-year increments for each of the 40 possible forecasts reveals: i) large spread in skill among the individual forecasts for any given year and ii) temporal variations in skill for each forecast. The magnitude of conditional prediction skill varies greatly from one year to the next, revealing that the boundary conditions offer little prediction skill during some years and comparably large skill during others. The simultaneous behaviors of the El Niño-Southern Oscillation and the subtropical Indian Ocean Dipole are related to the largest conditional precipitation prediction skill years. Unconditional skill estimates may therefore mislead users of forecasts who desire assessments of forecast accuracy. Unconditional skill may be temporally unstable, and unlike conditional skill, is not representative of the skill for a given season.

## 1. Introduction

### *1.1 Motivation*

The economic productivity of Southern Africa, defined herein as the African continent south of 15˚S (Fig.1), is closely related to weather and climate. Jury et al. (2002) estimated that 48% of the Southern Africa gross domestic product variance is explained by precipitation during the Austral summer rainy season. Rainfed agriculture is especially important to the Southern Africa economy, as it accounts for approximately 25% of the gross domestic product and employs nearly 70% of the labor force (Dixon et al. 2001). Large year-to-year precipitation variations during December-March (Fig. 1c), the core of the Southern Africa rainy season (Fig. 1b see also Mason and Jury 1997 and Hoell et al. 2017), can therefore shock the regional economy. Meager precipitation can lead to reduced agricultural production and reduced hydroelectric power generation while abundant precipitation can lead to flooding and damage to infrastructure (Conway et al. 2015).

Decision makers utilize predictions of December-March precipitation to better define, quantify and reduce the risk of future economic shocks over Southern Africa. Decision makers utilize outlooks issued by forecasters at many institutions, including National Meteorological and Hydrological Services, Regional Climate Outlook Forums, Drought Early Warning Systems and Famine Early Warning Systems (e.g. Hansen et al. 2011, Sheffield et al. 2014). Precipitation outlooks issued by these institutions are based on both statistical and dynamical forecasts. Statistical models have long been used to forecast Southern Africa precipitation, and generally leverage historical relationships between precipitation and variables elsewhere in the climate system (e.g. Hastenrath et al. 1995, Thiaw et al. 1999). Use of simulations from dynamical models have grown from a research activity to an operational pursuit over the past 30 years

(Weisheimer and Palmer 2014; Graham et al. 2011) to include forecast frameworks comprised of many different models; examples include, the North American Multi-model Ensemble (Kirtman et al. 2014), Copernicus Climate Service[2], Global Producing Centres for Long-Range Forecasts[3] and WMO Lead Center for Long-Range Forecasts Multi-Model Ensembles[4].

However, seasonal predictions alone do not provide enough information for decision makers, forecasters or forecast system developers. All three require an awareness of prediction accuracy, also known as prediction skill, in order to contextualize the prediction. Decision makers use prediction skill to establish if, when and where a seasonal prediction should be incorporated into practice across different economic sectors (Sarewitz et al. 2000, Hartmann et al. 2002). Forecasters use prediction skill in order to communicate the confidence in a given forecast. Forecast system developers use prediction skill to help guide possible forecast system improvements.

### *1.2 Prediction Skill Estimates*

Two types of prediction skill estimates have been developed to address user needs (e.g. Kumar 2007). One type is based on the verification of a series of predictions spanning many seasons. This type is an *unconditional* skill estimate since it is not specific to any boundary forcing. The other type is based on the verification of a single season. This type is a *conditional* skill estimate since it is dependent on the boundary forcing of a season.

Unconditional precipitation prediction skill is commonly expressed as the correlation of a series of forecasts with observations. An example of such a calculation is shown in Fig. 2a for January-March NMME forecasts made the previous December. The unconditional correlations

[2] https://climate.copernicus.eu/seasonal-forecasts
[3] http://www.wmo.int/pages/prog/wcp/wcasp/gpc/gpc.php
[4] https://www.wmolc.org/

between forecasts and observations during 1982-2009 of less than 0.10 suggest that the NMME forecast system has little skill in predicting Southern Africa precipitation during January-March at one-month lead.

There are a variety of ways to estimate conditional precipitation prediction skill, and we will show later that conditional skill is related to the occurrence probability of above, near and below average precipitation for a single season (e.g. Kumar 2007). In this construct, the proportion of individual forecasts from a prediction system that fall into above, near and below average bins constitute as the probability of that precipitation outcome. An example of such a calculation is shown in Fig. 2b for the January-March 2019 NMME precipitation forecast made the previous December. Below average precipitation probabilities between 40-50% over Southern Africa would lead one to believe that there is some confidence in the forecast of below average precipitation beyond chance. However, the confidence demonstrated by the probabilistic forecast in Fig. 2b is undermined by the low unconditional skill estimate shown in Fig. 2a.

To better inform Southern Africa decision makers and forecasters, we illustrate differences in unconditional and conditional seasonal precipitation prediction skill estimates over the region during December-March. Our methodology follows that of Kumar (2007). Unconditional and conditional prediction skill estimates are illustrated using a perfect-model experiment based on a 40-member ensemble of atmospheric model simulations forced by 1920-2016 observed time-evolving boundary conditions. The atmospheric model simulations are based on the Community Atmosphere Model version 5 (CAM5). We employ an atmospheric model instead of initialized coupled ocean-atmosphere forecast systems for two reasons. First, the atmospheric model isolates the prediction skill offered by SST. Second, the atmospheric model provides a long time series from which to evaluate prediction skill. In this application of the perfect-model, each ensemble member is selected as a proxy for observations while the average of the remaining members serves as the forecast for that observed proxy. This method generates many observed and forecast pairs for each of the 97 years examined.

The benefits of this analysis go beyond the interpretation of seasonal precipitation prediction skill estimates over Southern Africa. First, the use of atmospheric model simulations forced by the same boundary conditions enables an assessment of potential prediction skill, given that SSTs largely serve as the basis for seasonal prediction (e.g. Palmer and Anderson 1994). Second, the nearly 100-year focus period enables an assessment of whether precipitation prediction skill has changed in time, as suggested by Lawal et al. (2015) for the country of South Africa. Third, this analysis compliments assessments of the Southern Africa prediction skill in operational forecast systems (Landman and Beraki 2010, Yuan et al. 2014, Beraki et al. 2016, Landman et al. 2019). The hindcast periods and ensemble sizes of operational forecast systems tend to be much shorter and smaller, respectively, than the atmospheric model simulations that serves as the basis for the perfect-model method used here.

*1.3 Sources of Precipitation Prediction Skill*

We also use the conditional skill estimates based on the perfect-model method to objectively identify potential sources of December-March precipitation prediction skill and the mechanisms by which these sources drive Southern Africa precipitation. These conditional skill estimates can be used to establish how aspects of the boundary conditions may govern seasonal prediction skill without making prior assumptions on the sources of prediction skill.

Prior studies have largely isolated known modes of ocean-atmosphere variability and identified their relationships with Southern Africa precipitation. Most studies have focused on El

Niño-Southern Oscillation (ENSO) as a predictor (e.g. Hastenrath et al. 1995, Goddard and Dilley 2005, Manatsa et al. 2015), and to a lesser extent on predictors originating in the Indian Ocean, which include the Subtropical Indian Ocean Dipole (SIOD; e.g. Behera and Yamagata, Reason 2001, Washington and Preston 2006). Even fewer studies have focused on the combined effects of both ENSO and SIOD on Southern Africa precipitation (Hoell et al. 2016, 2017).

Research on the relationship between ENSO and Austral summer Southern Africa precipitation spans three decades (e.g. Nicholson and Entekhabi 1986, Ropelewski and Halpert 1987, 1989, Lindesay 1988). The two phases of ENSO, El Niño and La Niña, generally have opposing effects on Southern Africa climate (e.g. Jury et al. 1994; Rocha and Simmonds 1997; Nicholson and Kim 1997; Reason et al. 2000; Misra 2003). El Niño is related with below average precipitation due to high pressure, anomalous downward motion and reduced moisture fluxes into Southern Africa. By contrast, La Niña is related with above average precipitation due to low pressure, anomalous upward motion and enhanced moisture fluxes into Southern Africa. More recent research has examined the relationships between aspects of ENSO and Southern Africa precipitation. Different SST patterns associated with ENSO (e.g. Wyrtki 1975, Capotondi et al. 2014) are related with different atmospheric circulations over Southern Africa (Ratnam et al. 2014, Hoell et al. 2015). Also, stronger ENSO events are on average related with greater precipitation anomalies over Southern Africa (Pomposi et al. 2018).

The southwest-to-northeast oriented SST anomaly dipole over the Indian Ocean that is characteristic of the SIOD has been related with summertime Southern Africa precipitation (Behera and Yamagata, Reason 2001, Washington and Preston 2006). These SST anomalies have been found to modify the regional circulations over the southwestern Indian Ocean thereby affecting regional moisture fluxes that directly impact Southern Africa precipitation. The behavior of SIOD can complement or disrupt the Southern Africa precipitation relationship with ENSO (Hoell et al. 2016, 2017). When ENSO and SIOD are out of phase (e.g. El Niño and a negative SIOD or La Niña and a positive SIOD), Southern Africa on average experiences larger precipitation anomalies than if ENSO acted alone. When ENSO and SIOD are in phase (e.g. El Niño and a positive SIOD or La Niña and a negative SIOD), Southern Africa on average experiences lesser precipitation anomalies than if ENSO acted alone.

### *1.4 Paper Organization*

The organization of the paper is as follows. In section 2, the atmospheric model simulations and skill estimates derived from the perfect-model method are described. In section 3, we describe the behavior of seasonal conditional and unconditional prediction skill throughout the 20th and 21st centuries and discuss the sources of seasonal precipitation skill based on the conditional skill estimates. In section 4, we interpret differences in the prediction skill estimates and make recommendations for which skill estimate is most relevant to user needs.

## 2. Tools and Methods

### *2.1 Atmospheric Model Simulations*

The 40-member ensemble of atmospheric model simulations forced by an estimate of the observed time-evolving boundary conditions for 1920-2016 is based on CAM5 (Neale et al. 2012). The simulations utilize a finite volume dynamical core with horizontal resolution of 288 by 192 grid points in longitude and latitude, respectively, and 25 vertical levels. The boundary conditions that force each ensemble member include SSTs and sea-ice concentration from the merged Hadley (Rayner et al. 2003) -- NOAA Optimum Interpolation (Reynolds et al. 2007) data set constructed by Hurrell et al. (2008), greenhouse gases (Meinshausen et al. 2011), ozone (Lamarque et al. 2012) and aerosols (Tanre et al. 1984). While all ensemble members utilize analyzed SST, the weather for each member is different owing to their initializations from different atmospheric states in 1901. The simulations and further documentation can be obtained from http://www.esrl.noaa.gov/psd/repository/alias/facts/.

CAM5 simulates key features of the Global Precipitation Climatology Centre (GPCC, Schneider et al. 2014) observed estimate of areally averaged Southern Africa temporal precipitation variability south of 15˚S during December-March (Fig. 3). Another precipitation estimate, from the Climate Research Unit (CRU; Harris et al. 2014), is like GPCC over Southern Africa (Pomposi et al. 2018). The CAM5 ensemble mean precipitation appears to be correlated with the observed precipitation over prolonged periods (i.e. 1970s, 1990s and 2000s). The correlation between the two is 0.56 for the entire period of record. The ensemble mean filters atmospheric noise in each of the ensemble members, thereby reinforcing the ability of CAM5 to simulate relationships between the boundary conditions and Southern Africa precipitation highlighted by previous studies (Funk et al. 2018, Pomposi et al. 2018).

### *2.2 Prediction Skill Estimates Derived from the Perfect-Model Method*

The perfect-model method as applied here is a three-step process over which proxies of observed areally averaged Southern Africa precipitation time series and their forecasts during December-March are constructed from the atmospheric model simulations. The schematic of the atmospheric model simulations in Fig. 4, which is adapted from Kumar (2007), is used to describe the application of the perfect-model method. First, precipitation from a single member of the simulated ensemble is selected to proxy a time series of observations (columns in Fig. 4).

A single ensemble member and observations are conceptually similar since both are forced by a combination of internal weather/climate variations and the boundary conditions. Second, the remaining 39 ensemble members are averaged for each December-March season (rows in Fig. 4) to provide a simulated forecast of that observed time series. The averaging of the 39 members mutes the contribution of internal variability, and thereby reduces the temporal variations of each ensemble member. This makes clearer the effect of the prescribed boundary forcing in the atmospheric model. It is this boundary forcing that serves as the primary basis for seasonal prediction (e.g. Palmer and Anderson 1994). Third, steps one and two are repeated 40 times so every ensemble member serves as an observed proxy, resulting in 40 pairs of observed and forecast December-March Southern Africa time series for 1920-2016.

The proxies of observed and forecast December-March Southern Africa precipitation are used to calculate unconditional and conditional prediction skill. Anomaly correlation is the metric used to calculate skill though a variety of other skill measures could also be used. The skill calculations are based on the mathematical formulation outlined by Kumar (2007), which is repeated in the following.

December-March precipitation anomalies for each year and ensemble member in the atmospheric model simulations are obtained prior to calculating unconditional and conditional skill. Let $P_{i\alpha}$ denote precipitation for ensemble member $i$ and year $\alpha$. Precipitation anomalies for year $\alpha$ are calculated relative to a climatology. The climatology, $< P_\alpha >$, which depends on the year, is obtained from the average of the remaining years,

$$< P_\alpha > = \frac{1}{N(M-1)} \sum_j \sum_{\beta \neq \alpha} P_{j\beta} \tag{1}$$

where $N$=40 is the number of ensemble members and $M$=97 is the number of years. The anomaly for $P_{i\alpha}$ is then defined as

$$P'_{i\alpha} = P_{i\alpha} - < P_{\alpha} >. \tag{2}$$

This process is repeated until the precipitation anomaly for each year, $\alpha$, and ensemble member, $i$, is obtained.

Unconditional prediction skill is defined as the verification of one of 40 December-March forecast anomaly proxy time series, $O'_{i\alpha}$. For a randomly selected observed anomaly proxy time series, $I = i$,

$$O'_{I\alpha} = X'_{I\alpha}. \tag{3}$$

The corresponding forecast proxy, $F'_{I\alpha}$, of the observed anomaly proxy, $O'_{I\alpha}$, is obtained from the mean of the remaining 39 ensemble members,

$$F'_{I\alpha} = \frac{1}{N-1} \sum_{j \neq I} X'_{j\alpha}. \tag{4}$$

Unconditional skill in terms of anomaly correlation between the randomly selected observed and forecast proxy time series is defined by

$$Unconditional\ AC_I = \frac{\sum F'_{I\alpha} O'_{I\alpha}}{\sigma_I^F \sigma_I^O}. \tag{5}$$

where $\sigma_I^O$ and $\sigma_I^F$ are the standard deviations of the observed and forecast time series, respectively.

The unconditional skill calculation is repeated so each of the 40 ensemble members serves as a proxy for observations. We express unconditional skill in 30-year increments, for 30 years serve as the World Meteorological Organization recommendation for climate normals[5]. This allows for an assessment of how unconditional prediction skill may vary in time for the many possible evolutions of observed Southern Africa precipitation time series proxies.

Conditional prediction skill is defined as the verification of the many forecast proxies for a single December-March season. For a given year, $\alpha = A$, a randomly chosen observed anomaly proxy is represented by

$$O'_{iA} = X'_{iA}. \tag{6}$$

The corresponding forecast proxy, $F'_{iA}$, of the observed anomaly proxy, $O'_{iA}$, is obtained from the mean of the remaining 39 ensemble members

$$F'_{iA} = \frac{1}{N-1}\sum_{j \neq I} X'_{jA}. \tag{7}$$

This process is repeated 40 times to create pairs of observed and forecast precipitation proxies for each year. The conditional skill in terms of anomaly correlation for a given year is therefore

$$Conditional\ AC_A = \frac{\sum_i \ F'_{iA} O'_{iA}}{\sigma_A^F \sigma_A^F}. \tag{8}$$

---

[5] http://www.wmo.int/pages/prog/wcp/ccl/guide/documents/Normals-Guide-to-Climate-190116_en.pdf

The conditional skill calculation is repeated for each of the 97 December-March seasons. The magnitude of conditional prediction skill based on anomaly correlation is proportional to the magnitude of the signal-to-noise ratio, a common metric for assessing prediction skill conditioned on a specific boundary forcing (Fig. 5; see also Kumar and Hoerling 2000, Sardeshmukh et al. 2000). Signal-to-noise ratio is defined here as the ratio of the ensemble mean anomaly and the standard deviation of the ensemble.

Conditional skill is related to the probability of above, near and below average precipitation for a given season (e.g. Fig. 2), where each of those three categories refer to the upper, middle and lower terciles of the historical distribution of the model, respectively (Kumar 2009). The probabilities are obtained by binning Southern Africa precipitation in the CAM5 simulations. Tercile-based categorical probabilities are sometimes estimated using a Gaussian fitting method (e.g. Min et al. 2009). Such a method is not adopted here because we do not assume that Southern Africa precipitation follows a distribution.

### *2.3 Sources of Conditional Precipitation Prediction Skill*

Composites of SSTs, precipitation, 850 and 200 hPa winds and 500 hPa pressure vertical velocity based on discrete levels of conditional skill are used to objectively identify sources of December-March precipitation prediction skill and the mechanisms by which these sources drive Southern Africa precipitation. Four classes of conditional precipitation prediction skill are considered, when anomaly correlation skill falls between 0.25-0.50 and 0.50-1.0, for both above- and below-average precipitation forecasts. These conditional skill classes are chosen to align with signal-to-noise ratios of 0.5-1.0 and greater than 1.0 (Fig. 5). Signal-to-noise ratios of greater than 1.0 are often considered to be skillful since the ensemble mean anomaly exceeds one standard deviation (e.g. Kumar and Chen 2016). Above- and below-average forecast precipitation for a given December-March season are defined by the sign of the ensemble average precipitation anomaly of the model simulations.

## 3. Results

### *3.1 Unconditional Precipitation Prediction Skill*

The December-March Southern Africa seasonal unconditional precipitation prediction skill time series reveal two key characteristics of this skill type over the region (Fig. 6). First, the temporal characteristics of each of the 40 December-March forecast verifications are different, which highlights the combined effects of internal atmospheric behaviors and differences in the boundary forcing on 30-yr sequences of unconditional precipitation prediction skill (Kumar 2009). These variations in Southern Africa unconditional precipitation prediction skill through time could also lead to very different perceptions on the regional forecast skill, considering that such skill estimates of operational forecast models are based on a single observed trace of the climate.

Three examples of how unconditional precipitation prediction skill can vary in time are highlighted in Fig. 6: the verification based on GPCC in black, and two simulated verifications in pink and green. The forecast verification against GPCC tends to follow the behavior of many of the 40 members of the simulated proxies, with lower skill prior to 1970 and comparably higher skill thereafter. The green trace stands out among the members of the simulated ensemble, as the unconditional precipitation prediction skill with this chosen member as the proxy for verification is consistently much lower than all other ensemble members. The pink trace also stands out and is noteworthy for its exceptional decline in unconditional precipitation prediction skill from among the highest of the verifications around 2000 to among the lowest of the verifications in 2016.

The temporal variations across the 40 individual traces of unconditional precipitation prediction skill time series, as well as the verification based on GPCC, suggest a systematic increase in the magnitude of this skill estimate during 1920-2016. This increase is most evident in mean changes of 40 unconditional precipitation prediction skill estimates (Fig. 6 bold blue line), from about 0.40 anomaly correlation in the 1960s to about 0.55 anomaly correlation in 2016, after a maximum of near 0.65 anomaly correlation in 1990. Temporal variations in prediction skill across the 40 members is likely tied to changes in the behavior of the boundary forcing, given that the boundary forcing is the same across each of the members for the 30-year verifications. However, it is unclear whether such changes in unconditional skill are related to sustained or fleeting changes in the boundary forcing. It must be reiterated, however, that from the perspective of verification against an individual trace, year-to-year changes in unconditional precipitation prediction skill can be different from most of the other traces, an example of which was described by the green trace in Fig. 6.

For the second key characteristic, the spread among the 40 forecast verifications for any given year is large. The large spread highlights the effect of internal atmospheric variability on unconditional precipitation prediction skill, given that each observed proxy uses the same boundary conditions over the 30-year verification periods (Kumar 2009). This spread could therefore lead to very different perceptions of Southern Africa prediction skill and raises the question on how one should interpret unconditional precipitation prediction skill estimates.

The spread in unconditional precipitation prediction skill for given years is considered in the following examples. For the 30-year period ending in 1960, the average unconditional prediction skill for the 40 forecast verifications is 0.33 while the spread across the verifications is almost twice as large at 0.65 (Kumar 2009). Appreciable spread is also present during all other years, even 2000, the year during which the unconditional precipitation prediction skill spread was lowest and the mean skill highest. As pointed out by Kumar (2007), since correlation can only achieve a maximum value of 1, the spread and means of many unconditional skill estimates for a given year are inversely related. Also noteworthy is how the verification of a forecast based on GPCC always falls within the verification of model-based forecasts (Fig. 6 black line), which again suggests that the CAM5 atmospheric model with prescribed boundary conditions simulates realistic domain-average climate and prediction skill estimates over Southern Africa.

*3.2 Conditional Precipitation Prediction Skill*

Large interannual variability is the key characteristic of a seasonal December-March Southern Africa conditional precipitation prediction skill time series (Fig. 7), thus revealing the important effect of specific boundary forcing on the regional prediction skill for a given year. During some years the boundary conditions simply offer no precipitation prediction skill while during other years the boundary conditions offer comparably large precipitation prediction skill.

Interannual variability of the December-March Southern Africa conditional precipitation prediction skill can be drastic due to the amplitude of the predicted ensemble mean (Fig. 7). Examples of extreme year-to-year variations in which conditional skill moved from a bottom-5 to a top-5 season include 1972/73 to 1973/74, 1981/82 to 1982/83 and 1991/92 to 1992/93. The lack of year-to-year persistence in conditional precipitation prediction skill is further highlighted by the 0.01 lag-1 autocorrelation of the time series during 1920-2016. The sign alone of the precipitation anomaly forecast has no bearing on conditional precipitation prediction skill. The

Kolmogorov-Smirnov two-sample test indicates that distributions of forecast above and forecast below average precipitation are not statistically significant, with a p-value of 0.62. Above and below average forecast precipitation for a given December-March season are defined by the sign of the ensemble average precipitation anomaly of the model simulations.

The decade-to-decade variations in Southern Africa conditional precipitation prediction skill are also large (Fig. 7). This suggests that some knowledge of the boundary conditions over a sequence many years could provide an indication of the magnitude of precipitation prediction skill during that time. This compliments previous works that identified decadal variability in the time series of Southern Africa precipitation and its links to SSTs (e.g. Reason and Rouault 2002, Zhang et al. 2015, Dieppois et al. 2016). Conditional skill in these perfect-model simulations was comparably high during some decades, which include the 1960s, 1970s, 1980s and post-2000. By contrast, conditional skill was comparably low during other decades, which include the 1930s, 1940s, 1950s and 1990s. Interestingly, two standout conditional skill years did occur during those low skill decades; for example, 1938/39 and 1991/92.

The two decades spanning the 1960s and 1970s saw the largest magnitudes of December-March conditional precipitation prediction skill (Fig. 7). Above average precipitation forecasts prevailed during this span (Figs. 3 and 7), as the ensemble mean of the simulations was above average for 16 of those 20 years. Also, four of those above average forecast years ranked in the top 10 highest conditional precipitation prediction skill during 1920-2016.

The epoch spanning 1981/82 and 1991/92 also saw comparably high conditional precipitation prediction skill, but in contrast to the preceding two decades, the forecast during seven of those ten years was for below average precipitation (Figs. 3 and 7). The high skill during this epoch was bolstered by 3 of the top 11 skill years on record. While conditional skill during the post 2000 period lagged 1960-1990, 5 of the top 15 skill years showed up during that period associated with a below average precipitation forecast.

Larger magnitudes of December-March Southern Africa conditional precipitation prediction skill calculated via anomaly correlation are related to greater changes of the regional forecast precipitation distributions from climatology (Figs. 8 and 9). This underscores how particular configurations of the boundary conditions shape the probabilities of below, near and above average forecast seasonal precipitation in the presence of atmospheric noise (see also Fig. 2b). During instances of high conditional prediction skill, the boundary conditions provide an indication that forecast precipitation probabilities will differ from climatological probabilities (i.e. 33% for each below, near and above average seasonal precipitation) while during others the boundary conditions provide no such guidance.

Drastic shifts in the distributions of forecast December-March Southern Africa precipitation are related to conditional precipitation prediction skill that exceed 0.5 anomaly correlation (Fig. 9). While these instances are relatively uncommon, occurring just 15 times in 97 seasons, the forecasts reveal large changes in the odds of below or above average forecast precipitation outcomes. For the seven seasons during which the ensemble average is below average, the forecast distribution shifts appreciably to negative values, resulting in an 81% probability that precipitation is below average and just a 5% probability that precipitation is above average. For the eight seasons during which the ensemble average is above average, the forecast distribution shifts appreciably to positive values and narrows, resulting in a 73% probability that precipitation is above average and just a 3% probability that precipitation is below average.

Shifts in the distributions of forecast Southern Africa precipitation are also related to conditional precipitation prediction skill that fall between 0.25 and 0.5 (Fig. 9). These instances happen more often, occurring 23 times in 97 December-March seasons, and reveal important changes in the odds of either below or above average forecast precipitation outcomes. For the 12 seasons during which the ensemble average is below average, the distribution shifts to negative values, resulting in a 63% probability of below average precipitation and an 11% probability of above average precipitation. For the 11 seasons during which the ensemble average is above average, the distribution shifts to positive values and narrows, resulting in a 57% probability of above average precipitation and a 10% probability of below average precipitation.

*3.3 Sources of Conditional Precipitation Prediction Skill*

SST anomalies consistent with ENSO and SIOD are related to conditional precipitation prediction skill that exceed 0.5 anomaly correlation (c.f. Fig. 10a,b and Fig. 1 in Hoell et al. 2017), thus demonstrating that the greatest December-March Southern Africa precipitation prediction skill is obtained from simultaneous ENSO and SIOD events. The SST related to above and below average Southern Africa precipitation that meet the conditional skill criteria are mirror images. SST anomalies associated with above average Southern Africa precipitation are like El Niño and a negative SIOD (Fig. 10a) while SST anomalies associated with below average Southern Africa precipitation are like La Niña and a positive SIOD (Fig. 10b). The linearity in the SST relationships with Southern Africa precipitation is supported by Hoell et al. (2017, 2018) who showed that simultaneous ENSO and SIOD events are related to the greatest Southern Africa precipitation anomalies.

Southern Africa precipitation anomalies associated with high December-March conditional precipitation prediction skill are related to strong anomalies in the regional atmospheric circulation (Figs. 11a,b; 12a,b). Like the SST anomalies, anomalous atmospheric circulations related to above and below average Southern Africa precipitation that meet the conditional skill criteria are mirror images. Above average Southern Africa precipitation is related to anomalous low-level high pressure east of Madagascar, upper-level low pressure east of South Africa, anomalous onshore low-level winds, convergent low-level winds over land and anomalous mid-tropospheric downward motions over Southern Africa. Below average Southern Africa precipitation is related to anomalous low-level low pressure east of Madagascar, upper-level high pressure east of South Africa, anomalous offshore low-level winds, divergent low-level winds over land and anomalous mid-tropospheric downward motions over Southern Africa.

SST anomalies consistent with the SIOD are related to conditional precipitation prediction skill that falls between 0.25 and 0.50 anomaly correlation (c.f. Fig. 10c,d and Fig. 1 in Hoell et al. 2017), thus demonstrating December-March Southern Africa precipitation prediction skill is obtained from the SIOD alone. The SST related to above and below average Southern Africa precipitation that meet the conditional skill criteria are nearly mirror images, with SST dipoles in the southwest and central Indian Ocean (Fig. 10c,d). The southwestern Indian Ocean SST associated with below average Southern Africa precipitation is not clearly defined, likely as a result of warming SST over that region throughout the 1920-2016 period of record.

Southern Africa precipitation anomalies associated with December-March conditional precipitation prediction skill falling between 0.25 and 0.50 anomaly correlation are also related to anomalies in the atmospheric circulation (Figs. 11c,d; 12c,d). The anomalous atmospheric circulations follow similar patterns as the high conditional skill case described previously, but the magnitudes of the anomalies are not as strong.

## 4. Summary and Interpretation

### *4.1 Summary*

We illustrated herein the characteristics of unconditional and conditional seasonal precipitation prediction skill for Southern Africa during December-March, the core of the region's rainy season. Unconditional and conditional prediction skill were derived from the perfect-model method based on a 40-member ensemble of CAM5 simulations forced by observed time-evolving boundary conditions during 1920-2016. The perfect-model method was used to generate proxies of observed and forecast precipitation pairs from which forecast verifications using anomaly correlation were calculated.

The time series of Southern Africa conditional precipitation prediction skill varies strongly from one year to the next (Fig. 7), thus revealing the important effect of specific boundary forcing on the seasonal prediction skill for a given year. During some years the boundary conditions simply offer no precipitation prediction skill while during other years the boundary conditions offer comparably large precipitation prediction skill. Additionally, it was found that the magnitude of conditional precipitation prediction skill is related to changes in the distribution of forecast Southern Africa precipitation relative to a climatology, indicating that conditional skill estimates are implied by probabilistic seasonal forecasts (Fig. 9).

Time series of Southern Africa seasonal unconditional precipitation prediction skill reveal two key characteristics of this skill type over the region (Fig. 6). First, sequences of 30-year unconditional precipitation prediction skill verifications for each of the 40 individual traces of the climate vary differently in time. This temporal instability, also highlighted by Landman and Goddard (2002), underscores the combined effects of internal atmospheric behaviors and differences in the boundary forcing between verification periods. Second, the spread among each of the 40 forecast verifications during a given year is large, which underscores the effect of internal atmospheric variability on this skill type, given that each observed proxy is exposed to the same boundary conditions over the verification period.

We also used the conditional precipitation prediction skill estimates to objectively identify sources of seasonal precipitation prediction skill and the mechanisms by which those sources drive December-March Southern Africa precipitation (Figs. 10-12). Our methodology compliments many previous studies that isolated known modes of climate variability and identified links between those modes and Southern Africa. The simultaneous behaviors of ENSO and the SIOD offer the greatest conditional skill while a second tier of conditional skill is afforded by the SIOD alone.

*4.2 Interpretation*

The primary motivation for this analysis is to inform those interested in seasonal Southern Africa precipitation forecasts on the characteristics, strengths and weaknesses of two classes of widely-used prediction skill estimates. We hope that users will consider this information as they strive to make more informed decisions based on seasonal forecasts. We also hope that forecasters consider this information as they strive to express confidence, or lack thereof, in seasonal forecasts.

Unfortunately, the interpretation of prediction skill estimates by forecasters and decision makers is influenced by model biases. Model-based skill estimates rely on a model's rendition of how simulated interannual variability is separated into unpredictable and predictable components. For a single model like CAM5, the unpredictable component is dictated by the spread among the ensemble members, while the predictable component is dictated by the ensemble mean. Nonetheless, CAM5 has been found to simulate Southern Africa summertime precipitation adequately and we use it to diagnose the attributes of conditional and unconditional skill estimates.

We believe that the benefits of using conditional precipitation prediction skill estimates over Southern Africa overshadow the drawbacks. The primary feature of conditional skill is that it can distinguish between seasons during which there is no prediction skill and seasons during which there is comparably high prediction skill. This is a key attribute for a prediction skill estimate over a region like Southern Africa where the sources of the regional precipitation skill (i.e. ENSO and SIOD) are not active during some seasons. The inactivity of precipitation prediction skill sources during some seasons reduces the overall reliability of the forecast system, thereby making forecasts of opportunity as identified by conditional skill that much more important. Decision makers and forecasters can thereby decide as to whether a prediction for a given December-March season is meaningful and advise their audiences accordingly.

Conditional precipitation prediction skill has the attribute of being closely related to the probability distribution of forecast December-March Southern Africa precipitation. Greater shifts in the forecast precipitation anomaly distribution, resulting in changes to the probabilities of above or below average precipitation, are related to higher magnitudes of conditional skill. For an ensemble forecast system like NMME, where probabilistic forecasts are standard outputs (e.g. Fig. 2b), Southern Africa conditional precipitation prediction skill is implied. These shifts in probabilities can be used directly by users and forecasters to express confidence levels in a given seasonal forecast.

We believe that the drawbacks of using unconditional precipitation prediction skill over Southern Africa overshadow the benefits. The analysis of conditional skill strongly indicates important year-by-year variations in precipitation prediction skill that, by construct, unconditional precipitation prediction skill cannot distinguish since unconditional skill is based on a mixture of years with high and low conditional skill. Unconditional skill will in turn underestimate the prediction skill during seasons in which conditional skill is high and overestimate the prediction skill during seasons in which conditional skill is low. Unconditional skill therefore cannot provide guidance as to whether a skillful seasonal forecast during a given December-March season is expected.

Consider the following anecdote based on Fig. 2 that highlights how unconditional skill could undermine a rather confident probabilistic, or conditional, seasonal forecast. The verification of a history of past January-March forecasts made the preceding December suggests that NMME has little unconditional precipitation prediction skill over Southern Africa for that season (Fig. 2a). If a user were to ignore NMME forecasts entirely as a result of the unconditional skill estimate, they would also ignore that precipitation during some January-March seasons over Southern Africa are predictable. They would ignore that the January-March 2019 forecast is an example of such a season with prediction skill due to El Niño conditions, as evidenced by upwards of 50% probabilities of precipitation falling into the upper 33% of a historical distribution (Fig. 2b).

Also, unconditional precipitation prediction skill can be difficult to interpret for two reasons. First, there is large temporal instability of sequences of 30-year verifications for 40 individual traces of the climate. Second, the spread of unconditional prediction skill among the 40 traces of the climate for individual years is large. The pink and green traces in Fig. 6 are indicative of how a single evolution of the climate may greatly alter our perception the unconditional precipitation prediction skill. We oftentimes do not appreciate these possible variations in unconditional skill, since verifications of this type are typically made against a single observed time series for a temporally-limited hindcast period of an operational forecast model (e.g. 1982 and onward in Fig. 2a for NMME). This raises the question of whether the unconditional skill based on a single trace of the climate is suggestive of the true unconditional skill or is merely an outlier.

*Acknowledgements*

The authors are grateful for support from the Famine Early Warning Systems Network and constructive comments from Tom Hamill and two reviewers.

**References**


Beraki, A. F., W. A. Landman, D. DeWitt, and C. Olivier, 2016: Global dynamical forecasting system conditioned to robust initial and boundary forcings: seasonal context. International Journal of Climatology, 36, 4455-4474.

Capotondi, A., and Coauthors, 2014: Understanding ENSO Diversity. Bulletin of the American Meteorological Society, 96, 921-938.

Conway, D., and Coauthors, 2015: Climate and southern Africa's water–energy–food nexus. Nature Climate Change, 5, 837.

Dieppois, B., B. Pohl, M. Rouault, M. New, D. Lawler, and N. Keenlyside, 2016: Interannual to interdecadal variability of winter and summer southern African rainfall, and their teleconnections. Journal of Geophysical Research: Atmospheres, 121, 6215-6239.

Dixon, J., A. Gulliver, and D. Gibbon, 2001: Farming Systems and Poverty: Improving Farmers' Livelihoods in a Changing World. FAO and World Bank, 407.

Funk, C., and Coauthors, 2018: Examining the role of unusually warm Indo-Pacific sea-surface temperatures in recent African droughts. Quarterly Journal of the Royal Meteorological Society, 144, 360-383.

Goddard, L., and M. Dilley, 2005: El Niño: Catastrophe or Opportunity. Journal of Climate, 18, 651-665.

Graham, R. J., and Coauthors, 2011: Long-range forecasting and the Global Framework for Climate Services. Climate Research, 47, 47-55.

Hansen, J., S. Mason, L. Sun, and A. Tall, 2011: Review of seasonal climate forecasting for agriculture in Sub-Saharan Africa. Vol. 47, 205-240 pp.

Harris, I., P. D. Jones, T. J. Osborn, and D. H. Lister, 2014: Updated high-resolution grids of monthly climatic observations – the CRU TS3.10 Dataset. International Journal of Climatology, 34, 623-642.

Hartmann, H. C., T. C. Pagano, S. Sorooshian, and R. Bales, 2002: Confidence Builders. Bulletin of the American Meteorological Society, 83, 683-698.

Hastenrath, S., L. Greischar, and J. van Heerden, 1995: Prediction of the Summer Rainfall over South Africa. Journal of Climate, 8, 1511-1518.

Hoell, A., and L. Cheng, 2018: Austral summer Southern Africa precipitation extremes forced by the El Niño-Southern oscillation and the subtropical Indian Ocean dipole. Clim Dyn, 50, 3219-3236.

Hoell, A., C. Funk, T. Magadzire, J. Zinke, and G. Husak, 2015: El Niño–Southern Oscillation diversity and Southern Africa teleconnections during Austral Summer. Clim Dyn, 45, 1583-1599.

Jury, M. R., 2002: Economic Impacts of Climate Variability in South Africa and Development of Resource Prediction Models. Journal of Applied Meteorology, 41, 46-55.

Jury, M. R., C. Mc Queen, and K. Levey, 1994: SOI and QBO signals in the African region. Theor Appl Climatol, 50, 103-115.

Kirtman, B. P., and Coauthors, 2013: The North American Multimodel Ensemble: Phase-1 Seasonal-to-Interannual Prediction; Phase-2 toward Developing Intraseasonal Prediction. Bulletin of the American Meteorological Society, 95, 585-601.

Kumar, A., 2007: On the Interpretation and Utility of Skill Information for Seasonal Climate Predictions. Monthly Weather Review, 135, 1974-1984.

Kumar, A., 2009: Finite Samples and Uncertainty Estimates for Skill Measures for Seasonal Prediction. Monthly Weather Review, 137, 2622-2631.

Kumar, A., and M. P. Hoerling, 2000: Analysis of a Conceptual Model of Seasonal Climate Variability and Implications for Seasonal Prediction. Bulletin of the American Meteorological Society, 81, 255-264.

Kumar, A., and M. Chen, 2016: What is the variability in US west coast winter precipitation during strong El Niño events? Clim Dyn, 1-14.

Lamarque, J. F., and Coauthors, 2012: CAM-chem: description and evaluation of interactive atmospheric chemistry in the Community Earth System Model. Geosci. Model Dev., 5, 369-411.

Landman, W. A., and A. Beraki, 2010: Multi-model forecast skill for mid-summer rainfall over southern Africa. International Journal of Climatology, 32, 303-314.

Landman, W. A., and L. Goddard, 2002: Statistical Recalibration of GCM Forecasts over Southern Africa Using Model Output Statistics. Journal of Climate, 15, 2038-2055.

Landman, W. A., A. G. Barnston, C. Vogel, and J. Savy, 2019: Use of El Niño–Southern Oscillation related seasonal precipitation predictability in developing regions for potential societal benefit. International Journal of Climatology, 0.

Lawal, K. A., D. A. Stone, T. Aina, C. Rye, and B. J. Abiodun, 2015: Trends in the potential spread of seasonal climate simulations over South Africa. International Journal of Climatology, 35, 2193-2209.

Lindesay, J. A., 1988: South African rainfall, the Southern Oscillation and a Southern Hemisphere semi-annual cycle. Journal of Climatology, 8, 17-30.

Manatsa, D., T. Mushore, and A. Lenouo, 2015: Improved predictability of droughts over southern Africa using the standardized precipitation evapotranspiration index and ENSO. Theor Appl Climatol, 1-16.

Mason, S. J., and M. R. Jury, 1997: Climatic variability and change over southern Africa: a reflection on underlying processes. Progress in Physical Geography, 21, 23-50.

Meinshausen, M., and Coauthors, 2011: The RCP greenhouse gas concentrations and their extensions from 1765 to 2300. Climatic Change, 109, 213-241.

Min, Y.-M., V. N. Kryjov, and C.-K. Park, 2009: A Probabilistic Multimodel Ensemble Approach to Seasonal Prediction. Weather and Forecasting, 24, 812-828.

Misra, V., 2003: The Influence of Pacific SST Variability on the Precipitation over Southern Africa. Journal of Climate, 16, 2408-2418.

Neale, R. a. C., 2012: Description of the NCAR Community Atmosphere Model (CAM 5.0), 289 pp.

Nicholson, S., and D. Entekhabi, 1986: The quasi-periodic behavior of rainfall variability in Africa and its relationship to the southern oscillation. Arch. Met. Geoph. Biocl. A., 34, 311-348.

Nicholson, S. E., and J. Kim, 1997: The Relationship of the El Niño-Southern Oscillation to African Rainfall. International Journal of Climatology, 17, 117-135.

Palmer, T. N., and D. L. T. Anderson, 1994: The prospects for seasonal forecasting—A review paper. Quarterly Journal of the Royal Meteorological Society, 120, 755-793.

Pomposi, C., C. Funk, S. Shukla, L. Harrison, and T. Magadzire, 2018: Distinguishing southern Africa precipitation response by strength of El Niño events and implications for decision-making. Environmental Research Letters, 13, 074015.

Ratnam, J. V., S. K. Behera, Y. Masumoto, and T. Yamagata, 2014: Remote Effects of El Niño and Modoki Events on the Austral Summer Precipitation of Southern Africa. Journal of Climate, 27, 3802-3815.

Reason, C. J. C., and M. Rouault, 2002: ENSO-like decadal variability and South African rainfall. Geophysical Research Letters, 29, 16-11-16-14.

Reason, C. J. C., and D. Jagadheesha, 2005: A model investigation of recent ENSO impacts over southern Africa. Meteorol. Atmos. Phys., 89, 181-205.

Reason, C. J. C., R. J. Allan, J. A. Lindesay, and T. J. Ansell, 2000: ENSO and climatic signals across the Indian Ocean Basin in the global context: part I, interannual composite patterns. International Journal of Climatology, 20, 1285-1327.

Rocha, A., and I. A. N. Simmonds, 1997: Interannual variability of south-eastern African summer rainfall. Part 1: Relationships with air-sea interaction processes. International Journal of Climatology, 17, 235-265.

Ropelewski, C. F., and M. S. Halpert, 1987: Global and Regional Scale Precipitation Patterns Associated with the El Niño/Southern Oscillation. Monthly Weather Review, 115, 1606-1626.

——, 1989: Precipitation Patterns Associated with the High Index Phase of the Southern Oscillation. Journal of Climate, 2, 268-284.

Sardeshmukh, P. D., G. P. Compo, and C. Penland, 2000: Changes of Probability Associated with El Niño. Journal of Climate, 13, 4268-4286.

Sarewitz, D., R. A. Pielke Jr., and R. Byerly Jr., 2000: Prediction: Science, Decision Making, and the Future of Nature. Island Press, 405.

Schneider, U., A. Becker, P. Finger, A. Meyer-Christoffer, M. Ziese, and B. Rudolf, 2014: GPCC's new land surface precipitation climatology based on quality-controlled in situ data and its role in quantifying the global water cycle. Theor Appl Climatol, 115, 15-40.

Sheffield, J., and Coauthors, 2013: A Drought Monitoring and Forecasting System for Sub-Sahara African Water Resources and Food Security. Bulletin of the American Meteorological Society, 95, 861-882.

Tanre, D., J.-F. Geleyn, and J. M. Slingo, 1984: First Results of the Introduction of an Advance Aerosol-Radiation Interaction in the ECMWF Low Resolution Global Model. Aerosols and Their Climatic Effects, H. E. Gerber, and A. Deepak, Eds., Deepak, A., 133-177.

Thiaw, W. M., A. G. Barnston, and V. Kumar, 1999: Predictions of African rainfall on the seasonal timescale. Journal of Geophysical Research: Atmospheres, 104, 31589-31597.

Weisheimer, A., and T. N. Palmer, 2014: On the reliability of seasonal climate forecasts. Journal of The Royal Society Interface, 11.

Wyrtki, K., 1975: El Niño—The Dynamic Response of the Equatorial Pacific Ocean to Atmospheric Forcing. Journal of Physical Oceanography, 5, 572-584.

Yuan, C., T. Tozuka, W. A. Landman, and T. Yamagata, 2014: Dynamical seasonal prediction of Southern African summer precipitation. Clim Dyn, 42, 3357-3374.

Zhang, Q., K. Holmgren, and H. Sundqvist, 2015: Decadal Rainfall Dipole Oscillation over Southern Africa Modulated by Variation of Austral Summer Land–Sea Contrast along the East Coast of Africa. Journal of the Atmospheric Sciences, 72, 1827-1836.

**List of Figures**

Figure 1: For GPCC during 1920-2016, (a) average monthly precipitation (mm/day), (b) December-March annual precipitation contribution (percent) and (c) December-March precipitation coefficient of variation.

Figure 2: Precipitation prediction skill of the NMME forecast system available from http://www.cpc.ncep.noaa.gov/products/international/nmme/nmme.shtml. (a) Unconditional prediction skill of December-initialized January-March forecasts calculated through the correlation (times 100) of the forecast with observed precipitation during 1982-2009. (b) An approximation of conditional prediction skill for January-March 2019 forecasts initialized the previous December. These estimates are calculated by identifying the proportion of forecast members that fall into the above, near and below average terciles of the distribution of the forecast system.

Figure 3: Time series of December-March Southern Africa precipitation anomaly (mm/day). GPCC precipitation is shown in red, individual simulated ensemble members are shown in light blue and the simulated ensemble average is shown in dark blue. The correlation between GPCC and the simulated ensemble average is 0.56 ($p$<0.01).

Figure 4: Schematic diagram of the CAM5 simulations. The columns represent the different CAM5 ensemble members and the rows represent the December-March seasons. The schematic is adapted from Kumar (2007).

Figure 5: Scatter diagram of conditional skill (vertical axis) and signal-to-noise ratio (horizontal axis).

Figure 6: Time series of December-March Southern Africa 30-year end point unconditional precipitation prediction skill. Individual simulated ensemble members are shown in light blue, focus simulated ensemble members are shown in pink and green, the average of the 40 simulated ensemble members is shown in dark blue and GPCC precipitation is shown in black.

Figure 7: Time series of December-March Southern Africa conditional precipitation prediction skill. Green and brown bars indicate above and below average forecast precipitation. Above and below average precipitation are defined by the sign of the simulated ensemble average anomaly for a given season.

Figure 8: Scatter diagram of forecast December-March Southern Africa precipitation as a function of conditional precipitation prediction skill and the sign of the forecast ensemble average precipitation anomaly. The green and brown horizontal lines denote the thresholds for above and below average precipitation, respectively.

Figure 9: Box plot and the probability of forecast December-March Southern Africa precipitation falling below (brown), near (gray) and above (green) average as a function of conditional precipitation prediction skill and the sign of the forecast ensemble average precipitation

anomaly. Above and below average precipitation are defined by the sign of the simulated ensemble average anomaly for a given season. The tercile probabilities in the All category are 33.3%, but are shown here as 33% for clarity.

Figure 10: SST anomaly composite related to December-March Southern Africa conditional precipitation prediction skill and the sign of the ensemble average forecast precipitation. *n* denotes the number of seasons that qualify. SST is significant at the $p<0.05$ level based on a two-sided *t*-test.

Figure 11: Precipitation anomaly (mm/day) and 850 hPa wind anomaly (m/s) composites related to December-March Southern Africa conditional precipitation prediction skill and the sign of the ensemble average forecast precipitation. *n* denotes the number of forecasts included in the composite, equivalent to the number of qualifying seasons (see Figs. 8 and 9) over the 40 members of the ensemble. Precipitation is significant at the $p<0.05$ level based on a two-sided *t*-test.

Figure 12: 500 hPa pressure vertical velocity anomaly (hPa/day) and 200 hPa wind anomaly (m/s) composites related to December-March Southern Africa conditional precipitation prediction skill and the sign of the ensemble average forecast precipitation. *n* denotes the number of forecasts included in the composite, equivalent to the number of qualifying seasons (see Figs. 8 and 9) over the 40 members of the ensemble. Vertical velocity is significant at the $p<0.05$ level based on a two-sided *t*-test.

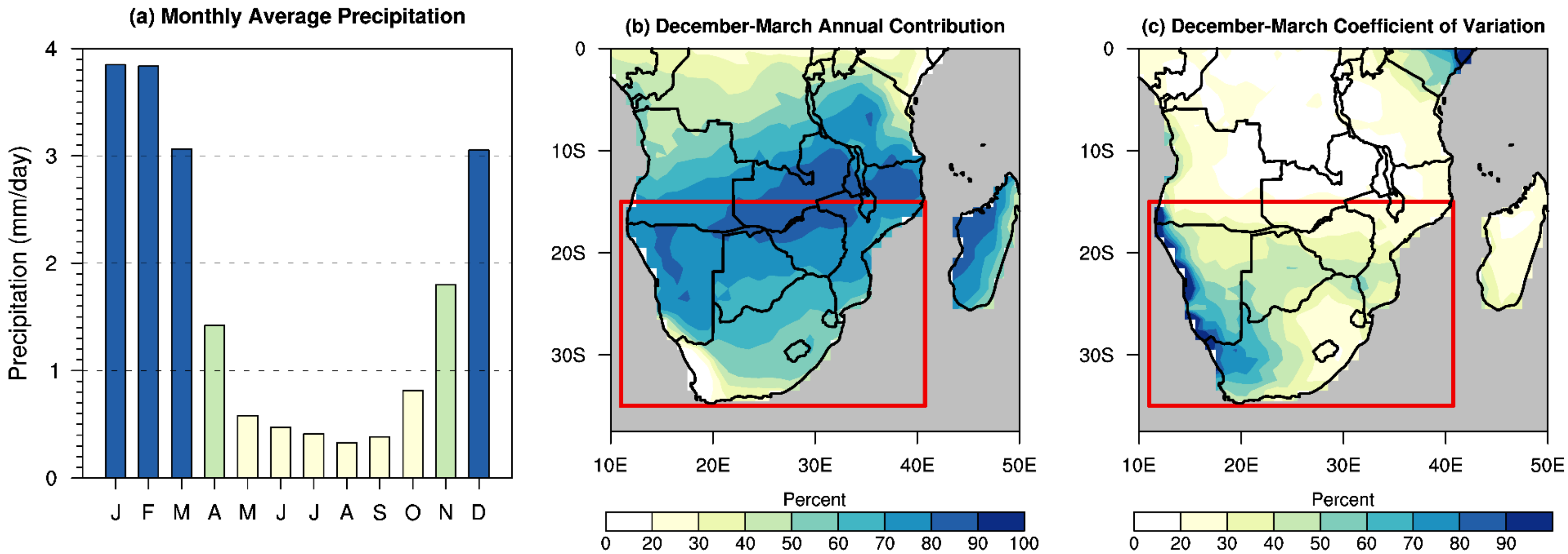


Figure 1: For GPCC during 1920-2016, (a) average monthly precipitation (mm/day), (b) December-March annual precipitation contribution (percent) and (c) December-March precipitation coefficient of variation.

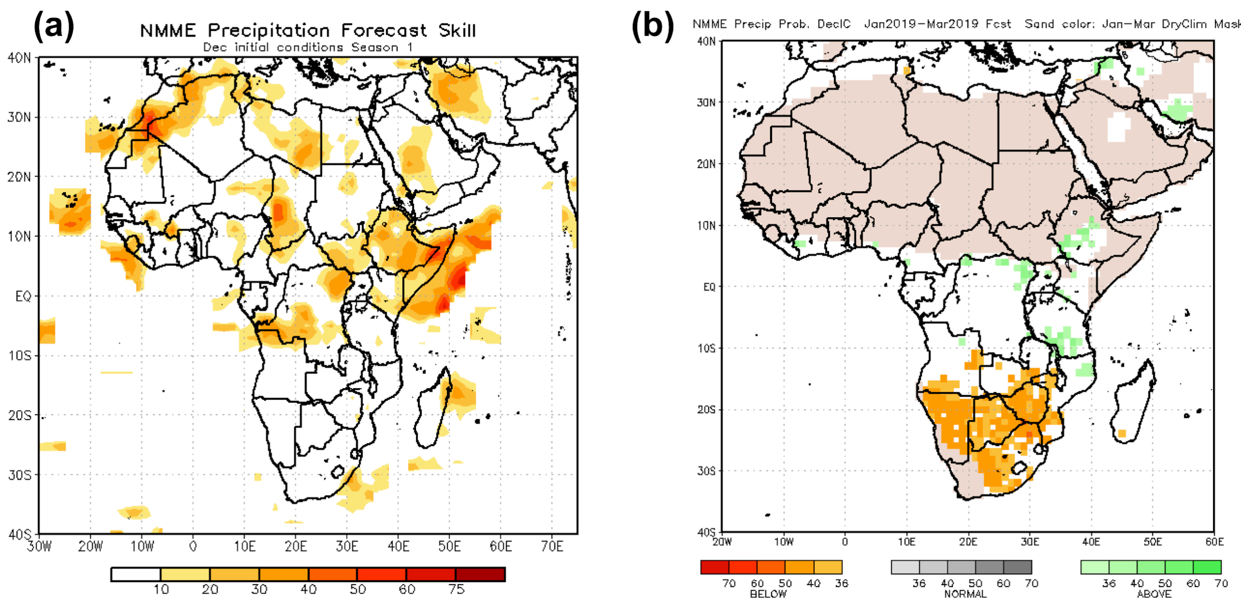


Figure 2: (a) Unconditional prediction skill of December-initialized January-March NMME forecasts calculated through the anomaly correlation (times 100) of the forecast with observed precipitation during 1982-2009. (b) Probabilistic forecasts of January-March 2019 precipitation initialized the previous December from NMME. These probabilistic forecasts are calculated by identifying the proportion of forecast members that fall into the above, near and below average terciles of the distribution of the prediction system. Both images were obtained from http://www.cpc.ncep.noaa.gov/products/international/nmme/nmme.shtml

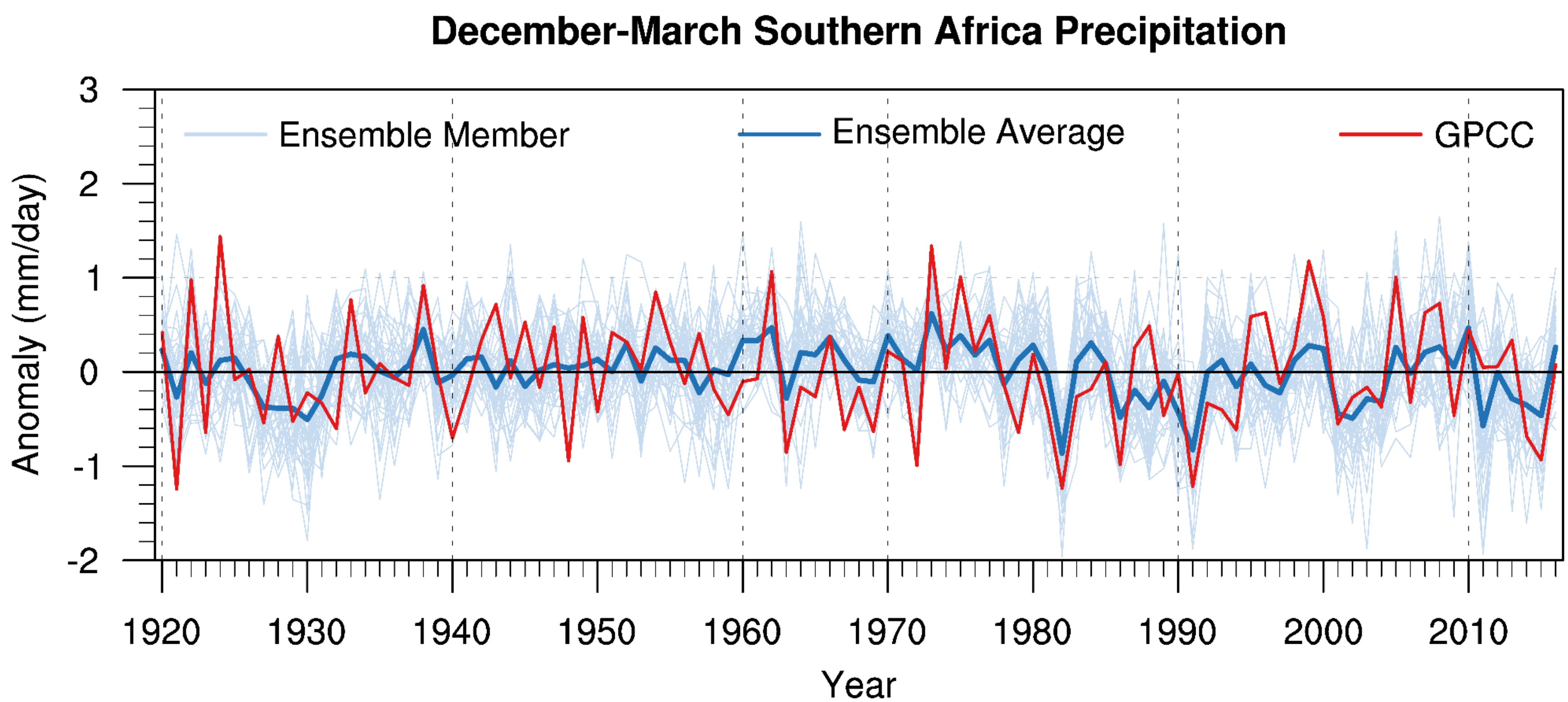


Figure 3: Time series of December-March Southern Africa precipitation anomaly (mm/day). GPCC precipitation is shown in red, individual simulated ensemble members are shown in light blue and the simulated ensemble average is shown in dark blue. The correlation between GPCC and the simulated ensemble average is 0.56 ($p$<0.01).

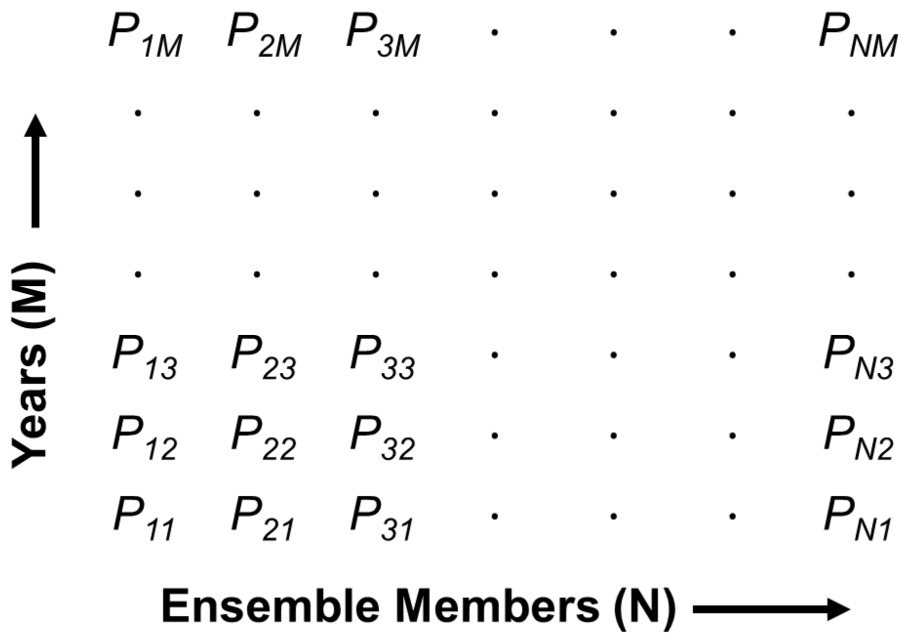


Figure 4: Schematic diagram of the CAM5 simulations. The columns represent the different CAM5 ensemble members and the rows represent the December-March seasons. The schematic is adapted from Kumar (2007).

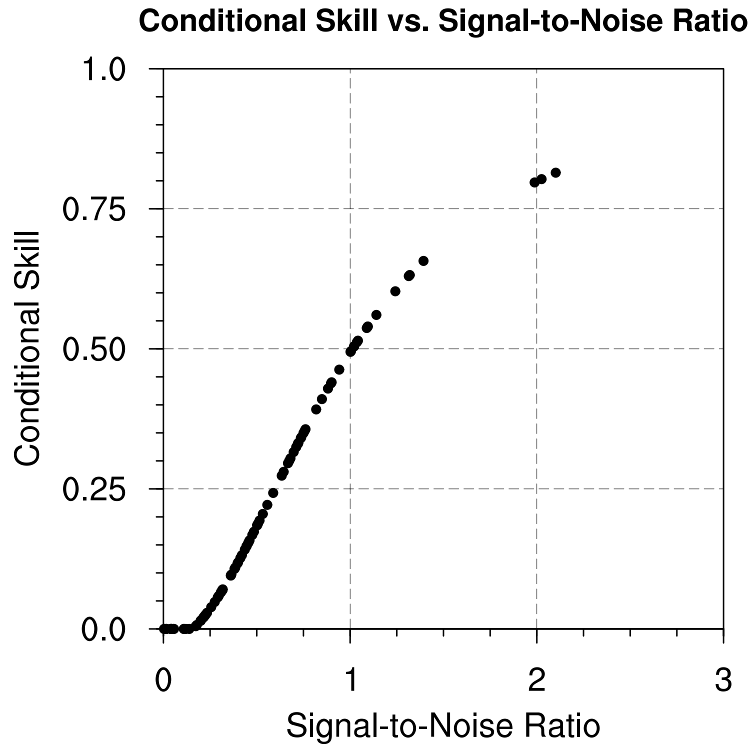


Figure 5: Scatter diagram of conditional skill (vertical axis) and signal-to-noise ratio (horizontal axis).

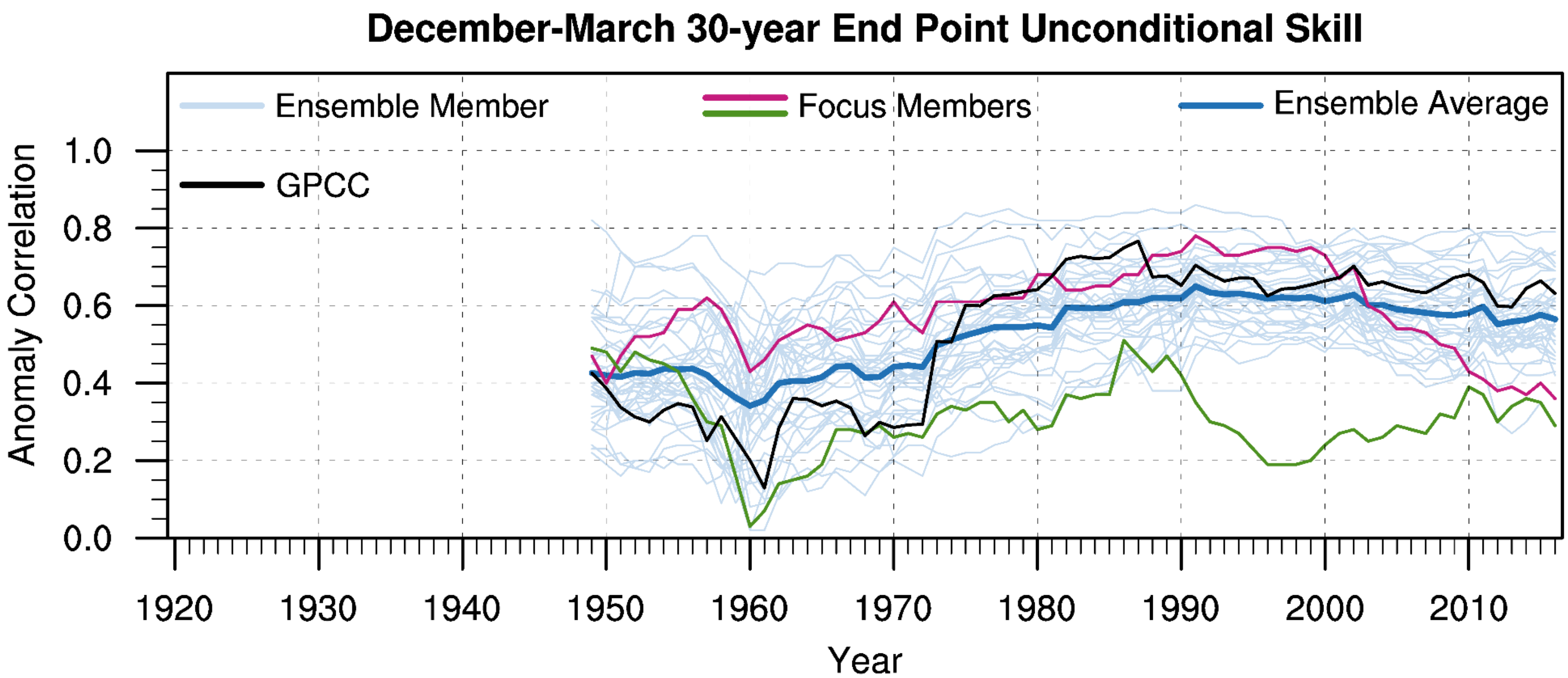


Figure 6: Time series of December-March Southern Africa 30-year end point unconditional precipitation prediction skill. Individual simulated ensemble members are shown in light blue, focus simulated ensemble members are shown in pink and green, the average of the 40 simulated ensemble members is shown in dark blue and the forecast verification against GPCC precipitation is shown in black.

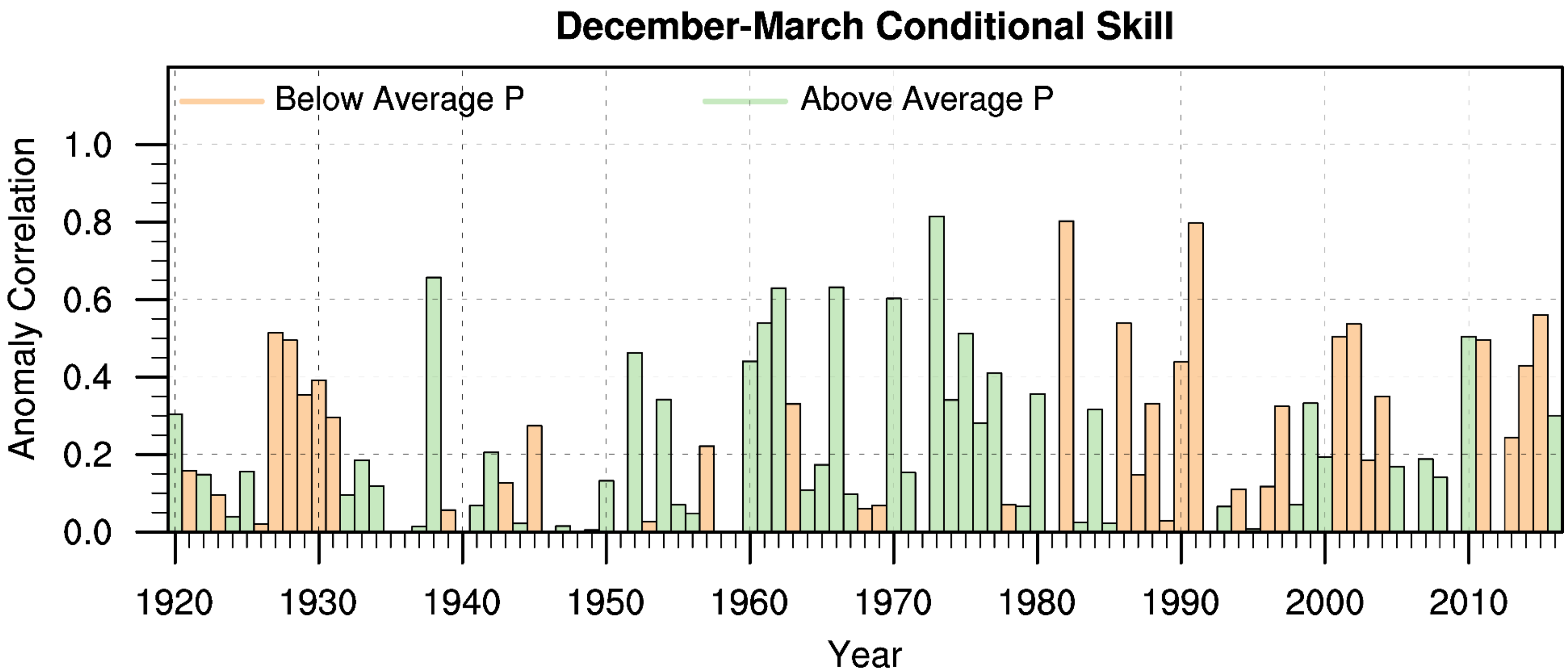


Figure 7: Time series of December-March Southern Africa conditional precipitation prediction skill. Green and brown bars indicate above and below average forecast precipitation. Above and below average precipitation are defined by the sign of the simulated ensemble average anomaly for a given season.

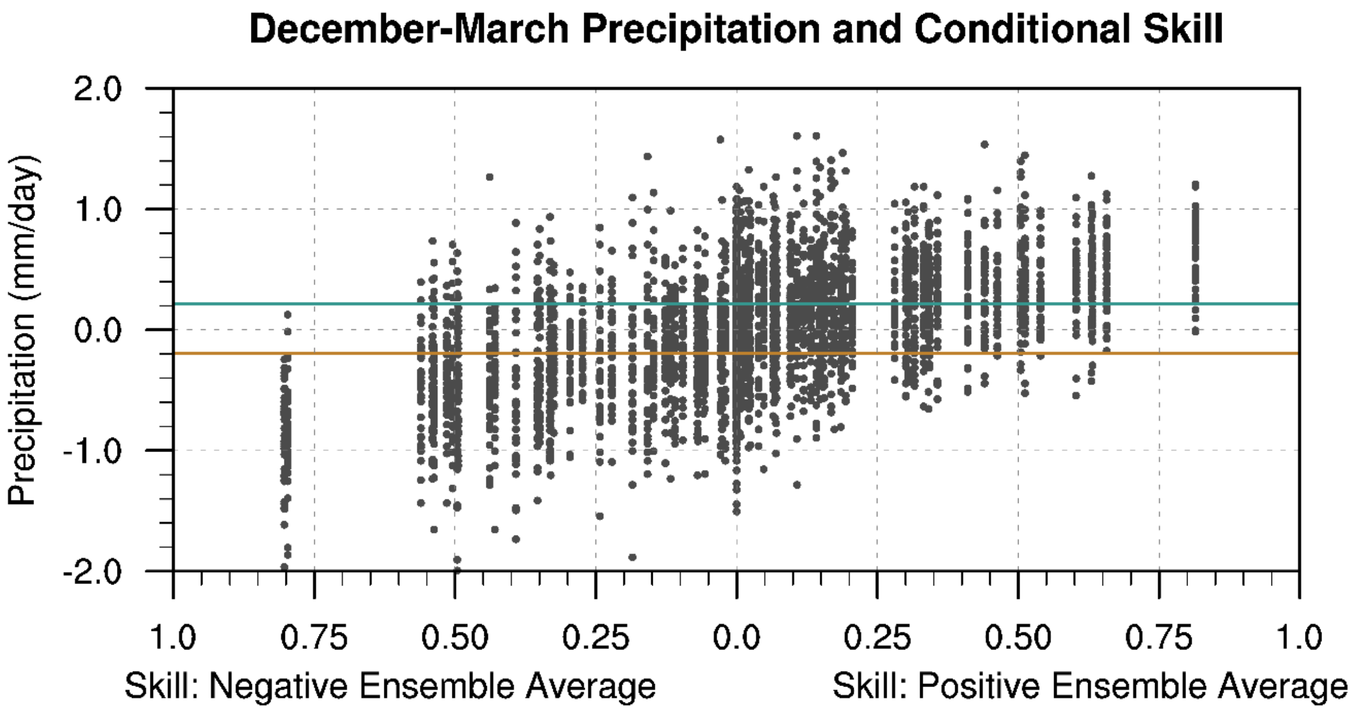


Figure 8: Scatter diagram of forecast December-March Southern Africa precipitation as a function of conditional precipitation prediction skill and the sign of the forecast ensemble average precipitation anomaly. The green and brown horizontal lines denote the thresholds for above and below average precipitation, respectively.

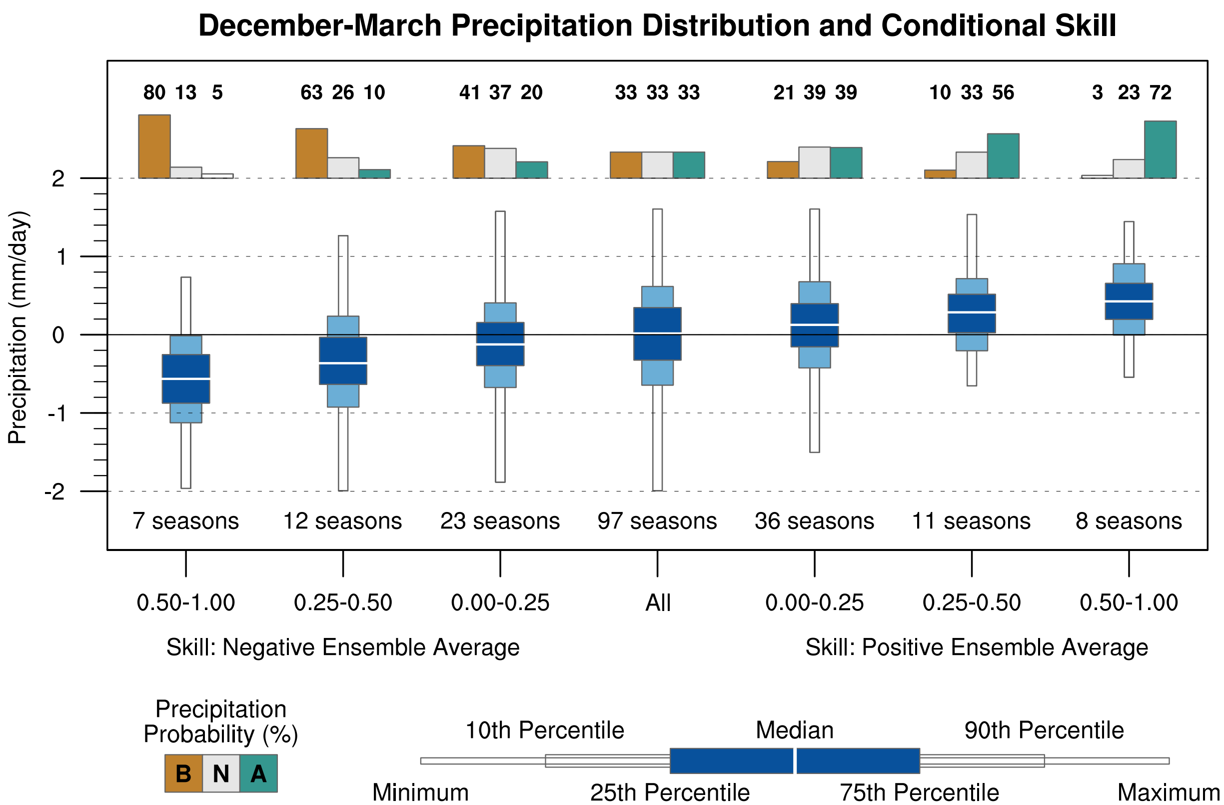


Figure 9: Box plot and the probability of forecast December-March Southern Africa precipitation falling below (brown), near (gray) and above (green) average as a function of conditional precipitation prediction skill and the sign of the forecast ensemble average precipitation anomaly. Above and below average precipitation are defined by the sign of the simulated ensemble average anomaly for a given season. The tercile probabilities in the All category are 33.3%, but are shown here as 33% for clarity.

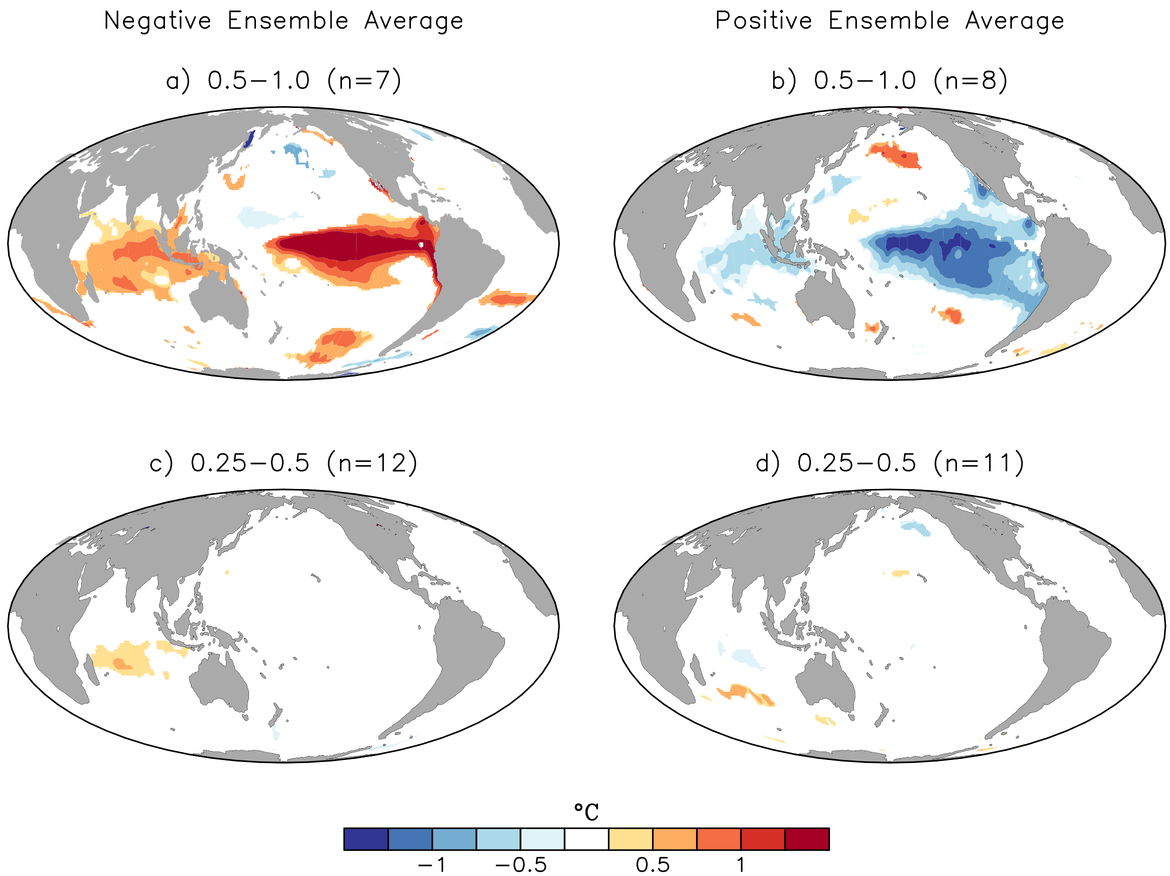


Figure 10: SST anomaly composite related to December-March Southern Africa conditional precipitation prediction skill and the sign of the ensemble average forecast precipitation. *n* denotes the number of seasons that qualify. SST is significant at the $p<0.05$ level based on a two-sided *t*-test.

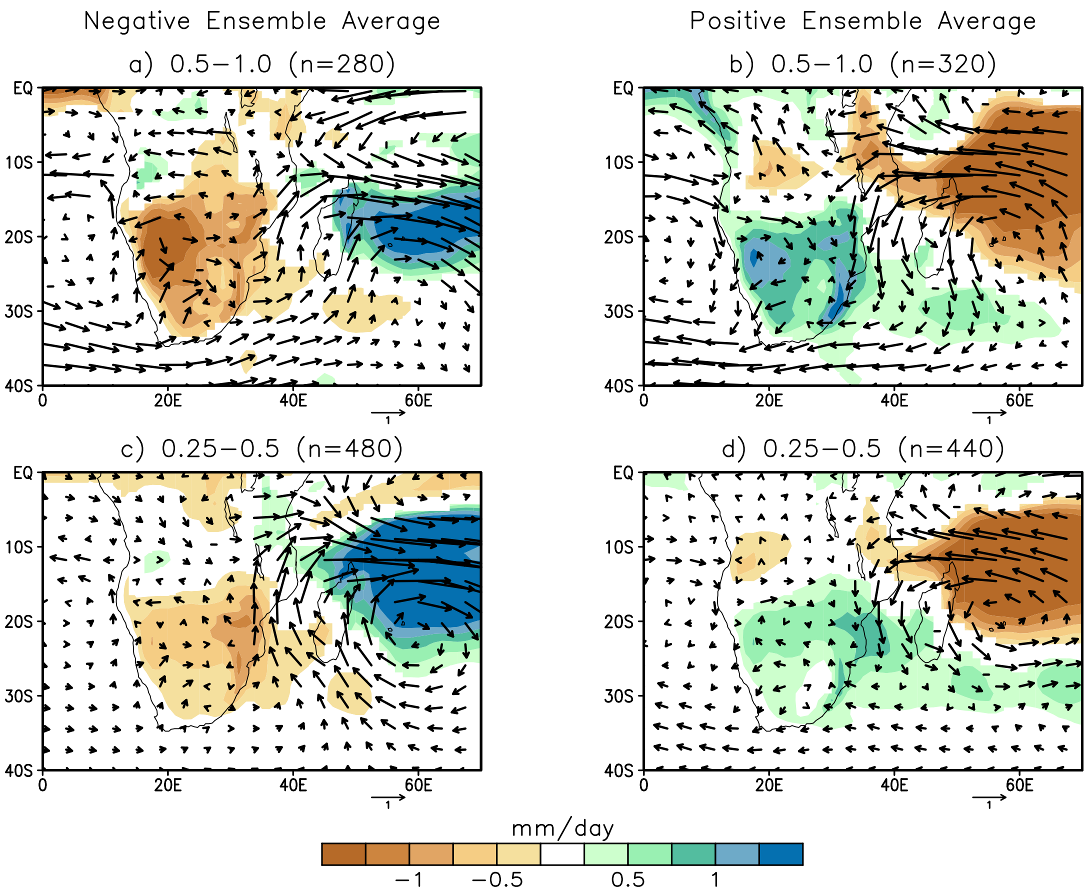


Figure 11: Precipitation anomaly (mm/day) and 850 hPa wind anomaly (m/s) composites related to December-March Southern Africa conditional precipitation prediction skill and the sign of the ensemble average forecast precipitation. *n* denotes the number of forecasts included in the composite, equivalent to the number of qualifying seasons (see Figs. 8 and 9) over the 40 members of the ensemble. Precipitation is significant at the $p<0.05$ level based on a two-sided *t*-test.

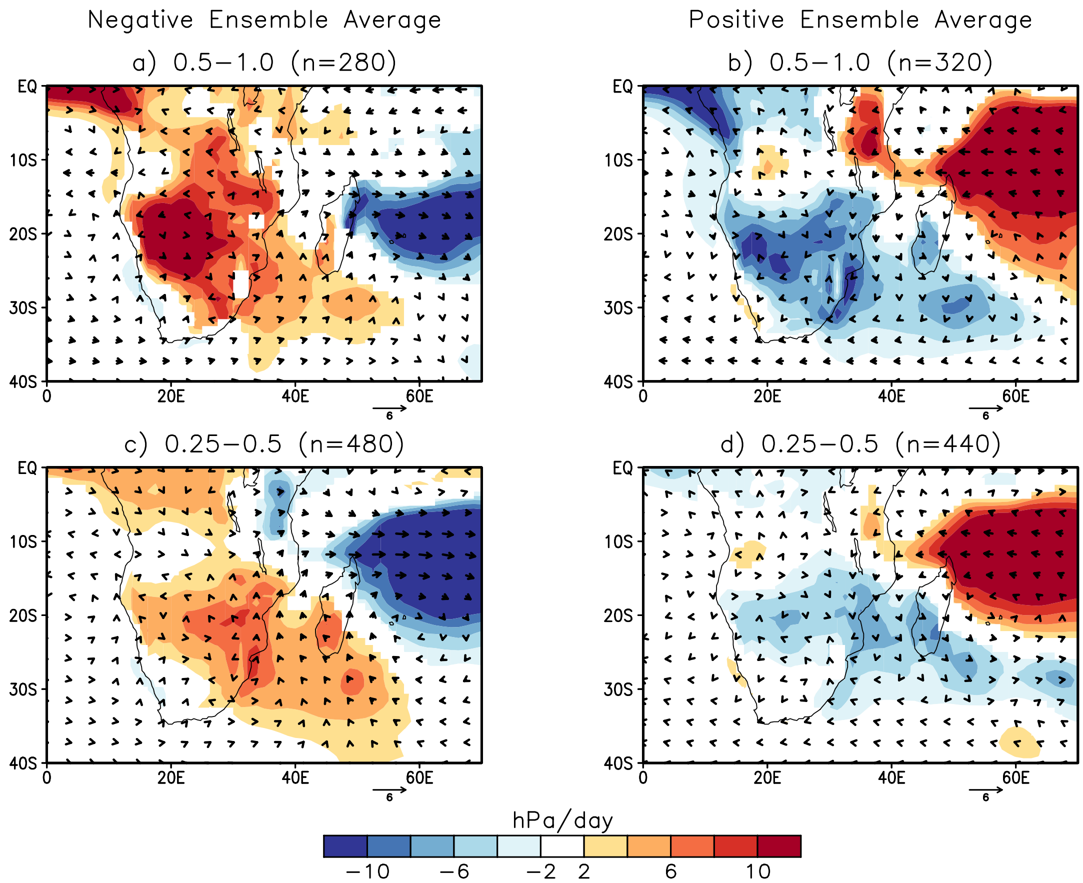


Figure 12: 500 hPa pressure vertical velocity anomaly (hPa/day) and 200 hPa wind anomaly (m/s) composites related to December-March Southern Africa conditional precipitation prediction skill and the sign of the ensemble average forecast precipitation. *n* denotes the number of forecasts included in the composite, equivalent to the number of qualifying seasons (see Figs. 8 and 9) over the 40 members of the ensemble. Vertical velocity is significant at the $p<0.05$ level based on a two-sided *t*-test.